An Improved Friction Model For Spark Ignition Engines

by

Daniel Sandoval

Submitted to the Department of Mechanical Engineering
in Partial Fulfillment of the Requirements for the Degree of
Bachelor of Science in Mechanical Engineering

at the

Massachusetts Institute of Technology

May 2002

Signature of Author.....
Department of Mechanical Engineering
May 10, 2002

Certified by.....
John B. Heywood
Sun Jae Professor of Mechanical Engineering
Thesis Supervisor

Accepted by.....
Ernest Cravalho
Chairman of the Undergraduate Thesis Committee
Department of Mechanical Engineering

AN IMPROVED FRICTION MODEL

FOR SPARK IGNITION ENGINES

by

Daniel Sandoval

Submitted to the Department of Mechanical Engineering
on May 10, 2002 in partial fulfillment of the
requirements for the Degree of Bachelor of Science in
Mechanical Engineering

Abstract

The details of a modified model that predicts friction mean effective pressure (fmep) for spark-ignition engines are described. The model, which was based on a combination of fundamental scaling laws and empirical results, includes predictions of rubbing losses from the crankshaft, reciprocating, and valvetrain components, auxiliary losses from engine accessories, and pumping losses from the intake and exhaust systems. These predictions were based on engine friction data collected between 1980 and 1989. Some of the terms are derived based on lubrication theory. Other terms are derived empirically from measurements of individual friction components, rather than the basic processes themselves. Current engine developments (improved oils, surface finish on piston liners, valve train mechanism) suggested that the model needed modification to predict modern engine losses due to friction. Modifications in oil viscosity, piston ring tension and gas pressure contribution on piston assembly, liner roughness, and valvetrain mechanism were made. The sum of the predictions now gives reliable estimates of spark-ignition engine fmep. The inclusion of oil viscosity scaling with temperature results in cold engine friction predictions about twice the value for warmed up engines. This agrees with the limited engine friction data used to modify the friction model.

Thesis Supervisor: John B. Heywood
Title: Sun Jae Professor of Mechanical Engineering
Director, Sloan Automotive Laboratory

Contents

List of Figures

List of Tables

Acknowledgements

I would like to thank Professor Heywood for giving me an opportunity to do research in engines. It was a great opportunity to work with such a knowledgeable patient, and supportive advisor. There were numerous times that he took the time to stay that extra time necessary to clarify any questions I had and to make sure I kept on going.

I would like to thank my parents. There are no words that can describe my appreciation for their love and the sacrifices they have made so that I can pursue my goals and aspirations. I have been extremely fortunate to have them in my life and thank them for their endless support and encouragement.

I thank everyone in the Sloan Automotive Lab, always willing to help me find information or understand certain concepts. In particular, Jenny Topinka, graduate student, and Dr. Tian Tian, for giving me guidance and advise throughout my work.

Thanks to the professional engineers in the automotive industry that guided me in understanding and interpreting the engine data.

1 Introduction

There is strong interest in improving spark-ignition and in reducing fuel consumption. For these reasons, it is of great importance to have accurate predictions of mechanical losses, a great part of which are friction losses due to the relative movement of adjacent components of the engine. Numerous publications have been made that detail measured and analysis based frictional losses incurred when running reciprocating engines. However, results are difficult to validate since the total friction loss is the summation of losses arising from many components in the engine. These friction components respond differently to variations of pressure, temperature, and speed as engine load varies [1].

The model for predicting "friction mean effective pressure" (fmep) described in this paper was developed to predict spark-ignition engine friction using basic engine design and operating parameters as inputs [2]. However, the data used to develop this model date back to the late 1980s. In order for this model to predict friction loses that occur in current engines, it was necessary to compare it to current engine friction data. This allowed an assessment and a recalibration of the friction terms in the model. Current engine friction data was used to determine the changes that needed to be made to certain constants in the model. The model was also expanded to include the lubricant viscosity in the model to include the effects of component temperature on the engine during cold start and warm-up transients. Finally, a comparison between pumping loses in the intake, exhaust, and the terms representing changes in cylinder gas pressure were made. The effect of these latter changes was minimal.

This thesis is organized as follows. A brief overview of the components of the engine friction model is presented, to explain what considerations were included in developing a friction model. The prior and improved models are then presented to show and explain the modifications that have been made to the friction terms. Data are then presented to compare the "old" and "new" model in a brief summary and the in a comparison of model breakdown against current engine friction data. Developing this model further, also allowed the effects of changing coolant temperature to examine the model effect of changing from start-up to warm-up conditions. Finally, a summary is presented to explain the improvements in the model and suggest some changes to keep it robust.

2. Engine Friction

2.1 Components of Engine Friction

Engine friction losses can be divided into three main categories: mechanical or rubbing losses, pumping losses, and auxiliary component losses. These losses are defined as follows [3]:

1. Rubbing losses or mechanical losses are those losses which result from relative motion between solid surfaces in the engine; i.e., the motion between a piston and a cylinder wall or a crankshaft journal and a main bearing. Relative motion does not require that the two solids be in contact with each other; in fact, it is generally the case that there is a film of lubricant between the surfaces.
2. Pumping losses are those losses associated with transporting fluids through the cylinder - made up of intake and exhaust pumping.
    a. Intake – Drawing the gas mixture through the intake system and into the cylinder.
    b. Exhaust – Expelling the burned gases from the cylinder and out of the exhaust system.
3. Auxiliary component losses are losses in driving engine accessories. These can include: the fan, the water pump, the oil pump, the fuel pump, the generator, a secondary air pump for emission control, a power-steering pump, and an air conditioner. Under most engine tests, the main accessories considered are those necessary for normal engine operation: the oil pump, the water pump, the fuel pump, and sometimes the alternator.

2.2 Measuring Friction

Two commonly used methods to obtain engine friction are "firing" and "motoring" of an engine. A true measurement of friction in a firing engine can be obtained by subtracting the brake mean effective pressure (output) from the indicated mep (energy transfer to each piston) determined from accurate measurements of cylinder pressure throughout the cycle. Pumping mep is obtained from the p-V data leaving mechanical and auxiliary friction losses. The second method is direct motoring of the engine, the engine is driven without firing, under conditions as close as possible to firing; for example, similar coolant temperature [3]. By motoring an engine and sequentially dismantling it, each component of mechanical friction contribution can be determined.

The motoring losses are different from the firing losses in terms of the gas loading on the piston, the piston and cylinder temperatures, and the exhaust blow down phase in the exhaust stroke. The lower gas loadings during motoring lower the rubbing friction. The temperatures are lower in a motoring test. Also, the gases in the exhaust phase are higher in density than under firing conditions [3].

3 Prior and Improved Friction Model

3.1 Background

The total engine friction prediction was defined as the sum of the predictions for mechanical, auxiliary, and pumping losses [2]. The rubbing and auxiliary losses were expressed as friction mean effective pressures, and the pumping loss was expressed as a pumping mean effective pressure, where *mean effective pressure,* mep, is defined as the work per cycle per unit of displaced volume:

$$mep = \frac{W_c}{V_d} \tag{1}$$

For individual rubbing friction interfaces and the auxiliary components, terms that related fmep to the basic engine design and operating parameters were developed. For the pumping loss, terms that related intake and exhaust system pressure drops to the appropriate design and operating parameters were developed. The resulting model was in the form:

$$tfmep = mfmep + afmep + pfmep \tag{2}$$

Relating rubbing interface fmep to design and operating parameters was a three-step process. First, an assumption that identified the type of lubrication present was made to determine the relationship between the friction coefficient and a dimensionless duty parameter, which was a function of viscosity (μ), velocity (V), and unit load (P). Figures 1 and 2 show the Stribeck diagram that plots friction coefficient vs. duty parameter, $\mu V/P$. There are three lubrication regimes that are important for engine components – boundary, mixed, and hydrodynamic lubrication. In boundary lubrication (no apparent lubrication) the friction coefficient is essentially constant. In mixed lubrication (some lubrication) the friction coefficient was assumed to vary inversely with engine speed. In hydrodynamic lubrication (full film lubrication) the friction coefficient was assumed to vary with a term proportional to the duty parameter [2].

The second and third steps in the rubbing friction term development were to use the friction coefficient to derive a term proportional to fmep for the interface in consideration and to "calibrate" the terms by multiplying them by constants based on empirical results. Patton explained the detailed analysis used to derive the terms, and used friction data for individual engine components and groups to calibrate these terms.

The auxiliary and pumping fmep terms were independent of lubrication. These terms are explained in Section 3.3.1, Component Breakdown.

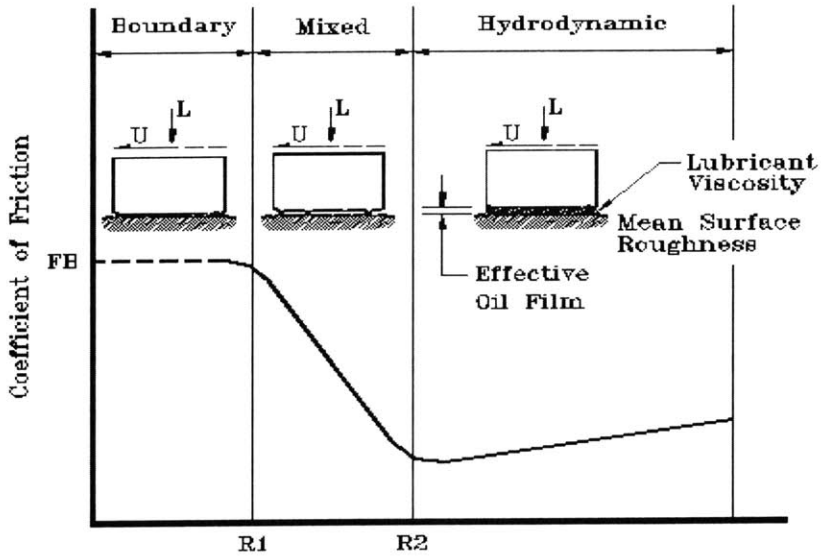

DUTY PARAMETER μV/P

Variable Description:

FB Coefficient of friction for boundary lubrication.

R1 Ratio of effective oil film to surface roughness when boundary lubrication begins.

R2 Ratio of effective oil film to surface roughness when mixed lubrication begins.

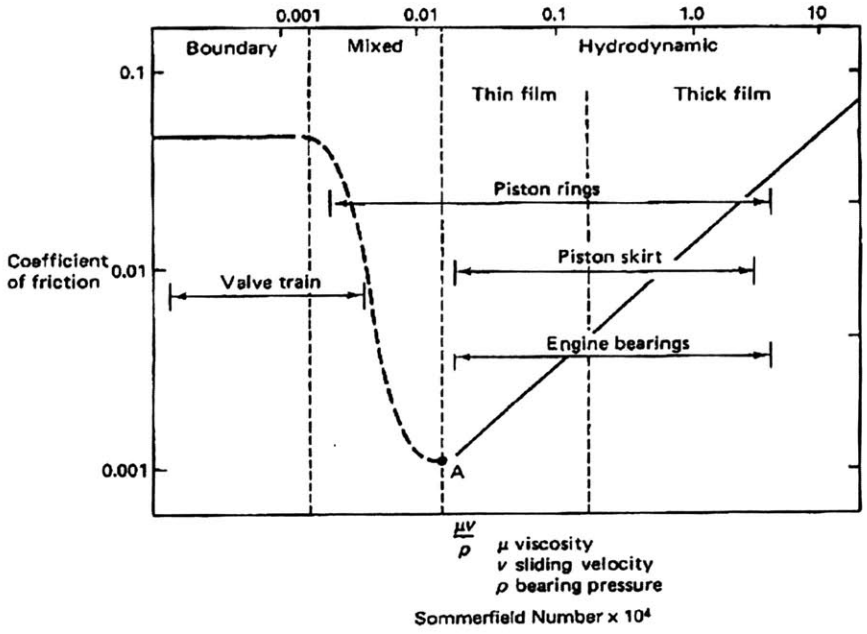

Figures 3-1 and 3-2: Stribeck Diagram –Lubrication Regimes. Figures from [4] and [5]

3.2 Modification of Friction Model

The purpose of this investigation was to determine how well the friction model predicted friction for current engines to then improve the predictive accuracy of the model. Engine development has significantly improved engine performance and efficiency over the past 10 years or so. Modifications in oil viscosity, crankshaft bearings and seals, piston design, piston ring design, liner roughness, and valvetrain mechanism, have decreased the total amount of friction losses in modern engines [1].

The improvements made in the friction model were made knowing that the friction work components fall under three main categories: those that are independent of speed (boundary friction), proportional to speed (hydrodynamic friction), or those proportional to speed squared (turbulent dissipation). Other components are a combination of these [3].

Literature on engine lubrication suggested that the hydrodynamic terms in the model should be modified to compensate for the differences between oil grades and the temperature dependence of engine oil viscosity. The fundamental literature for tribology of reciprocating engines shows that the viscosity scaling that should be included in the hydrodynamic friction terms has the form [6]:

$$\mu_{scaling} = \sqrt{\frac{\mu(T)}{\mu_o(T_o)}} \tag{3}$$

where $\mu(T)$ is the viscosity of the oil in the engine for which friction predictions are being made, and $\mu_o(T_o)$ is the reference viscosity for the engines that provided the data used to calibrate the model when it was first developed. Patton's paper [2] indicates that a reference 10W30 oil was used (viscosity 10.6 cSt at 90°C) in obtaining the engine data he used. This falls in the midrange of current oil grades used in engines. Table 1, shows current typical viscosity data for different oil grades:

Table 3.1: Typical Test Data for Oil Viscosity [7]

Oil Grade	**5W-20**	**5W-30**	**10W-30**	**10W-40**	**20W-50**
CPS Number	220135	220013	220019	220059	220060
Viscosity, Kinematic					
cSt at 40°C	49.2	66.1	74.8	98.9	174.4
cSt at 100°C	8.6	11	10.8	14.4	19.1

A more detailed set of oil grades that listed kinematic viscosity ν is given in the Appendix A.2. Since the relationship between ν and μ is a scaling factor, which is constant density, Equation 3 was written as:

$$\mu_{scaling} = \sqrt{\frac{\nu(T)}{\nu_o(T_o)}} \tag{4}$$

where ν(T) is the viscosity of the oil in the engine that is being tested, and ν_0(T) is the reference viscosity at reference temperature T_0. The Vogel equation, which gives the relation between temperature and low shear kinematic viscosity, was used in the form [8]:

$$\nu_0 = k \exp\left(\frac{\theta_1}{\theta_2 + T}\right) \tag{5}$$

where ν_0 is the kinematic viscosity of the low shear rate oil in cSt, and k(cSt), θ_1(°C) and θ_2(°C) are correlation constants for an oil and T is the oil temperature in °C. Furthermore, the low shear rate viscosity was multiplied by a ratio of μ_∞/μ_0 to convert to the high shear rate kinematic viscosity used in the model. This was done because most of the engine components operate at a high shear range where multi grade oils exhibit shear thinning.

$$\nu = \nu_0\left(\frac{\mu_\infty}{\mu_0}\right) \tag{6}$$

The oil grades and constants used are listed in the Appendix A.2 [8].

Modifications in the boundary and mixed lubrication terms were also made. The terms in each component of the friction model that were changed, and the explanation for that change, are detailed in the following section.

3.3 Component Friction Models

The following sections describe each term in the crankshaft, reciprocating, valvetrain, auxiliary, and pumping models. Each section describes the lubrication regime that was used to develop the terms for each model and the modifications made to each term. A detailed explanation on the derivation of each term can be found in Patton [2]. The definitions of all symbols and the expression for the total fmep are included in the Appendix A.1 and A-2.

3.3.1 Component Breakdown

1. Rubbing friction was divided into three component groups:

   Crankshaft – Main bearings, front and rear main bearing oil seals.

   Reciprocating – Connecting rod bearings, pistons, and piston rings.

   Valvetrain – Camshafts, cam followers, and valve actuation mechanisms.

2. Pumping losses were:

   Intake system, intake and exhaust valve(s), and exhaust system.

   Turbulent dissipation in hydrodynamic journal bearings (in rubbing friction component).

3. Auxiliary losses were:

Oil pump, water pump and alternator (necessary for normal engine operation).

* A cross sectional view of an engine showing the components is found in the Appendix A-1.

3.3.2 Crankshaft Friction

Crankshaft friction was estimated by adding a prediction of front and rear main bearing seal friction to a prediction of main bearing friction. The main bearing friction prediction included a hydrodynamic journal bearing term and a turbulent dissipation term, the latter accounting for losses due to the transport of oil through the bearings. The three terms that make up the crankshaft friction were:

$$cfmep = 1.22\times10^{5}\left(\frac{D_b}{B^2 S n_c}\right)+3.03\times10^{-4}\left(\frac{ND_b^3 L_b n_b}{B^2 S n_c}\right)+1.35\times10^{-10}\left(\frac{D_b^2 N^2 n_b}{n_c}\right) \qquad (7.a)$$

The first term gave the friction of the main bearing seals. The seals were assumed to operate in the boundary lubrication regime due to direct contact between the seal lips and the crankshaft. The seal lip load was assumed constant. The second term was for the main bearing hydrodynamic friction - derived using the friction coefficient for hydrodynamic lubrication. The last term accounted for the turbulent dissipation, the work required to pump fluids through flow restrictions [3].

Modifications

The only modification made to the crankshaft friction model was to include the viscosity scaling in the hydrodynamic friction term.

$$cfmep = 1.22\times10^{5}\left(\frac{D_b}{B^2 S n_c}\right)+3.03\times10^{-4}\sqrt{\frac{\mu}{\mu_o}}\left(\frac{ND_b^3 L_b n_b}{B^2 S n_c}\right)+1.35\times10^{-10}\left(\frac{D_b^2 N^2 n_b}{n_c}\right) \qquad (7.b)$$

3.3.3 Reciprocating Friction

The reciprocating component group friction prediction included piston, piston ring, and connecting rod friction. Piston ring friction was divided into two terms; one that predicted friction for the piston rings without gas pressure loading, and one that predicted the increase in piston ring friction caused by gas pressure loading. The resulting friction terms were:

Terms without gas pressure loading

$$rfmep = 2.94\times10^{2}\left(\frac{S_p}{B}\right)+4.06\times10^{4}\left(1+\frac{1000}{N}\right)\left(\frac{1}{B^2}\right)+3.03\times10^{-4}\left(\frac{ND_b^3L_bn_b}{B^2Sn_c}\right) \quad (8.a)$$

The first term gives the piston friction assuming hydrodynamic lubrication. The second term is for the piston ring friction term developed assuming mixed lubrication. The function, 1+1000/*N*, was selected to make the friction coefficient decrease by a factor of 2.5 from low to high speeds. The last term accounts for the hydrodynamic journal bearing fmep term for connecting rod bearings. This term is the same as the term for the main bearings in Equation 7.a.

Terms with gas pressure loading

$$rfmep_{gas} = 6.89\frac{p_i}{p_a}\left[0.088r_c + 0.182r_c^{\left(1.33-KS_p\right)}\right] \quad (9.a)$$

The term for piston ring friction due to gas pressure loading used the product of intake pressure (p_i) and a factor which included compression ratio (r_c) raised to constant – relating to the physics of the compression process.

Modifications

There were several modifications made to the piston terms, as there have been considerable improvements in piston rings and liner to reduce the amount of friction between these two surfaces.

Terms without gas pressure loading

$$rfmep = 2.94\times10^{2}\sqrt{\frac{\mu}{\mu_O}}\left(\frac{S_p}{B}\right)+4.06\times10^{4}\left(\frac{F_t}{F_{to}}C_r\right)\left(1+\frac{500}{N}\right)\left(\frac{1}{B^2}\right)+3.03\times10^{-4}\sqrt{\frac{\mu}{\mu_O}}\left(\frac{ND_b^3L_bn_b}{B^2Sn_c}\right) \quad (8.b)$$

For the equation without gas pressure effect, the viscosity scaling was incorporated into the piston friction and connecting rod bearing hydrodynamic terms. For the piston ring friction term, three modifications were made. Two factors, piston ring tension and surface roughness, were included to take into account a decrease in piston friction due to these two terms. Although studies have been made to measure these contributions, the improvements can only be accounted on a case-by-case basis. For this study, the engine data for piston friction was used to give a value to these terms. The last change was to decrease the value of the function, 1 +1000/N to 1 +500/N, to make the friction coefficient decrease by a factor of 1.8 instead of 2.5, which affects the friction coefficient for boundary lubrication.

Terms with gas pressure loading

$$rfmep_{gas} = 6.89 \frac{p_i}{p_a}\left[0.088\sqrt{\frac{\mu}{\mu_O}}r_c + 0.182\left(\frac{F_t}{F_{to}}\right)r_c^{(1.33-2KS_p)}\right] \quad (9.b)$$

For the equation with gas pressure effect, the viscosity scaling was included in the first term. For the second term, the piston ring tension factor was also included. For the exponential term, the constant K was doubled to reflect a reduction in liner roughness.

3.3.4 Valve Train Friction

The valvetrain component friction prediction included estimates of camshaft, cam follower, and valve actuation mechanism friction for a variety of valvetrain configurations. Flexibility dictated that the model be general enough to predict friction for multiple types of interfaces, yet selective enough to include only the effects of specific components for a desired valve configuration. The terms modeled camshaft bearing hydrodynamic friction, cam follower friction for flat or roller followers, oscillating hydrodynamic friction, and oscillating mixed lubrication. The resulting terms were:

$$vfmep = 244\frac{Nn_b}{B^2Sn_c} + C_{ff}\left(1+\frac{1000}{N}\right)\frac{n_v}{Sn_c} + C_{rf}\left(\frac{Nn_v}{Sn_c}\right) + C_{oh}\left(\frac{L_v^{1.5}N^{0.5}n_v}{BSn_c}\right) + C_{om}\left(1+\frac{1000}{N}\right)\frac{L_v n_v}{Sn_c} \quad (10.a)$$

The first term gave the camshaft bearing hydrodynamic friction. This term had a form similar to those of the main and connecting rod journal bearing terms. Engine data indicated that some of the friction was independent of piston speed (extrapolation back to zero engine speed gave a nonzero fmep value), so a constant 4.12 kPa was added to the camshaft bearing term. The constant value represented the boundary-lubricated friction due to the camshaft bearing seals. The next two terms predicted friction resulting from relative motion between the cam lobe and the cam follower. The second term predicted friction in the mixed lubrication regime for flat follower configurations. The third term predicted rolling contact friction for roller follower configurations. The fourth term, oscillating hydrodynamic friction, predicts friction caused by relative motion between relative motion between valvetrain components whose lubrication states were either completely or partially hydrodynamic, such as the valve lifter in the lifter bore or the valve in the valve guide The constants for the valvetrain terms (C_{ff}, C_{rf}, C_{oh}, C_{om}) were dependent on the type of valvetrain configuration being modeled. The values of the constants for SOHC-finger flat and

roller follower configurations were obtained using engine data. The values for the constants for other valve train configurations were estimated as fractions of the SOHC constants.

Modifications

There were two main modification made to the valve train friction terms. The first was including the viscosity scaling in the camshaft bearing and oscillating hydrodynamic friction terms. The second, was to lower the value of the function, 1 +1000/N to 1 +500/N, in the flat follower and oscillating mixed lubrication term.

$$vfmep = 244\sqrt{\frac{\mu}{\mu_o}}\frac{Nn_b}{B^2 Sn_c} + C_{ff}\left(1+\frac{500}{N}\right)\frac{n_v}{Sn_c} + C_{rf}\left(\frac{Nn_v}{Sn_c}\right) + C_{oh}\sqrt{\frac{\mu}{\mu_o}}\left(\frac{L_v^{1.5}N^{0.5}n_v}{BSn_c}\right) + C_{om}\left(1+\frac{500}{N}\right)\frac{L_v n_v}{Sn_c} \quad (10.b)$$

3.3.5 Auxiliary Friction

The auxiliary component friction prediction was an estimate of the sum of oil pump, water pump, and non-charging alternator friction. All of the auxiliary component fmep were assumed to be proportional to engine displacement. The auxiliary fmep model was:

$$afmep = 6.23 + 5.22\times10^{-3}N - 1.79\times10^{-7}N^2 \quad (11)$$

The constants were determined from a group of small, high-speed diesel engines. The negative coefficient for the engine speed squared term resulted from a gradual leveling off of oil pump fmep; typically, as oil pressure reaches its limited value in the middle speed range, less work is required of the pump.

Modifications

There were no modifications made in the auxiliary components losses since the terms were only dependent on engine speed. Also, there was not enough information available to determine properties of the components being tested in the first set of engines or in the engine data used to modify the model.

3.3.6 Pumping Losses

The pumping loss model predicted intake and exhaust pumping mean effective pressure (pmep).

Pumping work for either the intake or exhaust strokes was defined as the difference between cylinder pressure and atmospheric pressure, integrated over the volume of the intake or exhaust stroke. The intake and exhaust terms are listed below.

Intake

$$pmep_i = (p_a - p_i) + 4.12 \times 10^{-3} \left(\frac{p_i}{p_a} \right)^2 \left(\frac{S_p^2}{n_v^2 r_i^4} \right) \tag{12}$$

The first term for the intake pmep was assumed to be equal to the sum of the intake manifold vacuum and the intake valve pressure drop term. Intake manifold vacuum was calculated directly as the difference between atmospheric and intake pressure ($p_a - p_i$). The second term measured intake valve pressure drop.

Exhaust

$$pmep_e = 0.178 \left(\frac{p_i}{p_a} S_p \right)^2 + 4.12 \times 10^{-3} \left(\frac{p_i}{p_a} \right)^2 \left(\frac{S_p^2}{n_v^2 r_e^4} \right) \tag{13}$$

The first term in the exhaust model measured the exhaust system pressure drop. It was derived to measure typical production engine systems. The second term measured exhaust valve pressure drop.

Modifications

The constant for both valve pressure drop terms in Patton's model was based on results for diesel engines. The assumption that had been made was that pmep for SI engines was similar to pmep for diesel engines. Results from motoring tests of SI engines have indicated that the constant may have been too high. In this modified model, the constant for the valve pressure drop was changed to 3.0 $x10^{-3}$ kPa-s^2/m^2, following Patton's suggestion. The smaller constant may also take into account improvements in intake manifold design. With this change, the model gave a more accurate prediction for the intake and exhaust losses.

3.4 Comparison of Prior and Improved Model

Figure 3-3, shows the friction values for each friction component model for the 5.4L engine. The last three columns show the total mechanical, pumping, and total friction mean effective pressure. The total mechanical column was the sum of the first five columns and the total friction column included the pumping losses. The modified total friction model expression was included in Appendix A-2.

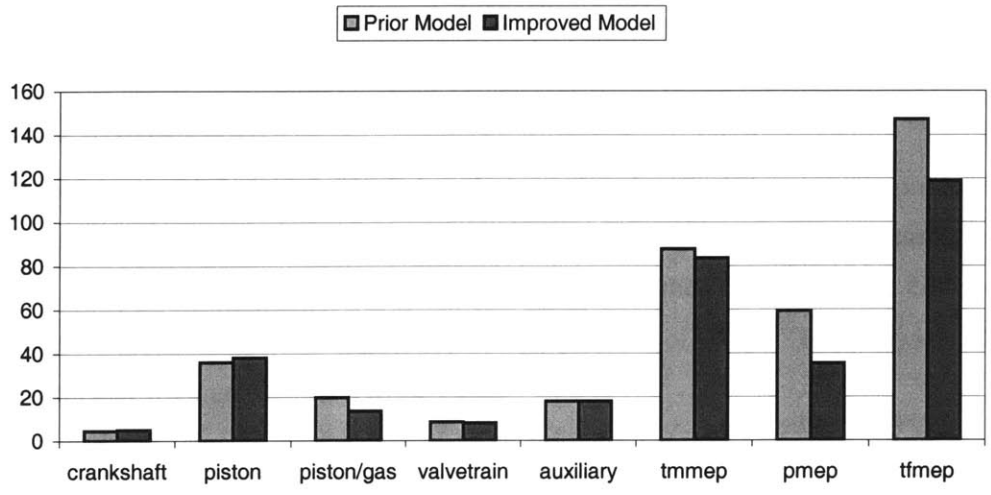

Figure 3-3: Friction Data for 5.4L Engine at 2500 rpm - WOT

No large differences can be seen in the mechanical friction models (crankshaft, piston, piston/gas, and valvetrain) since the viscosity scaling was only included in the hydrodynamic terms – which make a small contribution to the total value of friction for each of these models. However, there is a difference of about 6 kPa in the piston/gas term due to the piston ring tension, surfaces roughness, and mixed lubrication factors that were included in that model. The auxiliary losses were the same since the model was not modified. For the pumping model, the change made to the valve pressure drop constant decreased the pumping loss distribution by 25 kPa.

4 Results

Section 4.1 lists the three engines (5.4L, 3.0L, and 6.8L) that were used to validate and compare the changes that were made to the friction model. The first two engines were used to test the mechanical friction model. The last engine was used to test the pumping losses model. A comparison between the model and data for the 5.4L and 3.0L engine is presented to explain each friction model. The prototype engine was used to compare the pumping loss model at varying intake pressures. The rest of the sections will show the results for the improved friction model.

4.1 Engine Parameters

The modifications to the friction model were based on friction data from two current production engines and a prototype engine. The two current production engines were tested by motoring. This gave component friction data that allowed us to modify and compare the results for each component of the model. The engines were tested at an engine coolant temperature of 90^0C. The following table lists the engine parameters that were used in the friction model.

Table 4.1: Engines Parameters

Engine Type	Current	Current	Prototype
Engine	5.4L	3.0L	6.8L
Engine Information			
Layout/ # Cylinders	V8	V6	V10
Valves/Cylinder	2	4	
Valvetrain Type	SOHC	DOHC	SOHC
Valvetrain Mechanism	Direct Acting	Roller Finger Follower	Roller Finger Follower
Bore/Stroke Ratio	0.85	1.1	0.9
Compression Ratio	9.0	10.0	11.75

4.2 Crankshaft Friction

Figures 4-1 and 4-2, show that the improved friction model gave the same trend but significantly under predicted the crankshaft friction measurement for both engines. The crankshaft terms may oversimplify the complexity of modeling the crankshaft friction, since about 80% of the friction was accounted for by the hydrodynamic and turbulent dissipation terms. It also may be that testing the crankshaft without the pistons and connecting rods significantly increased the friction since the counter weights offset the balance of the crankshaft under these conditions.

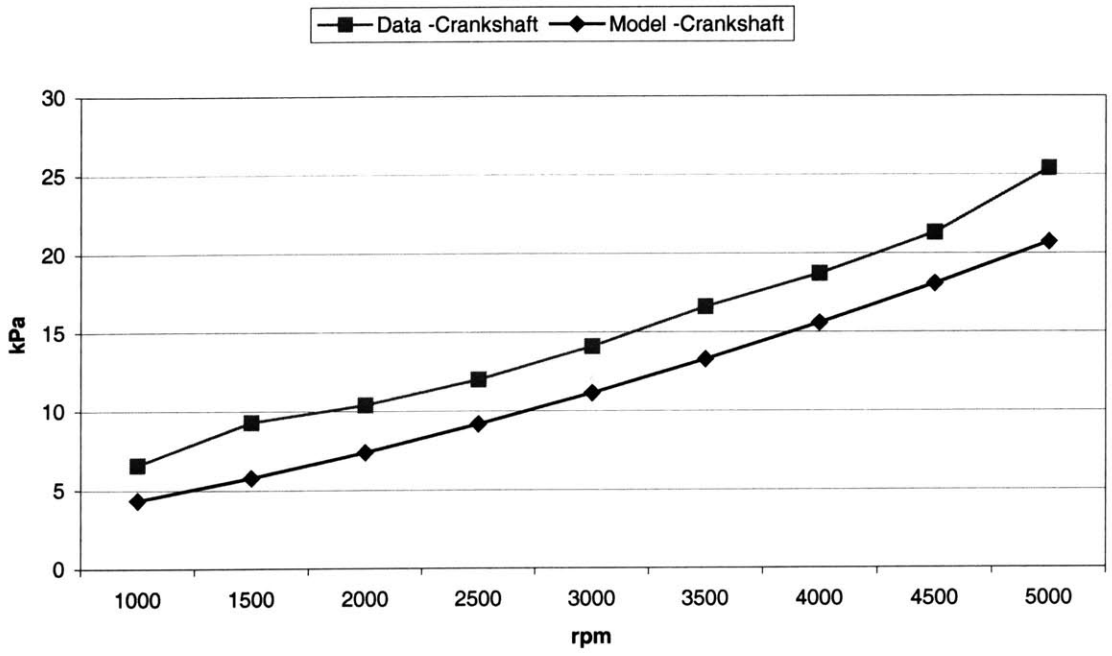

Figure 4-1: Comparison of crankshaft friction for 3.0L engine

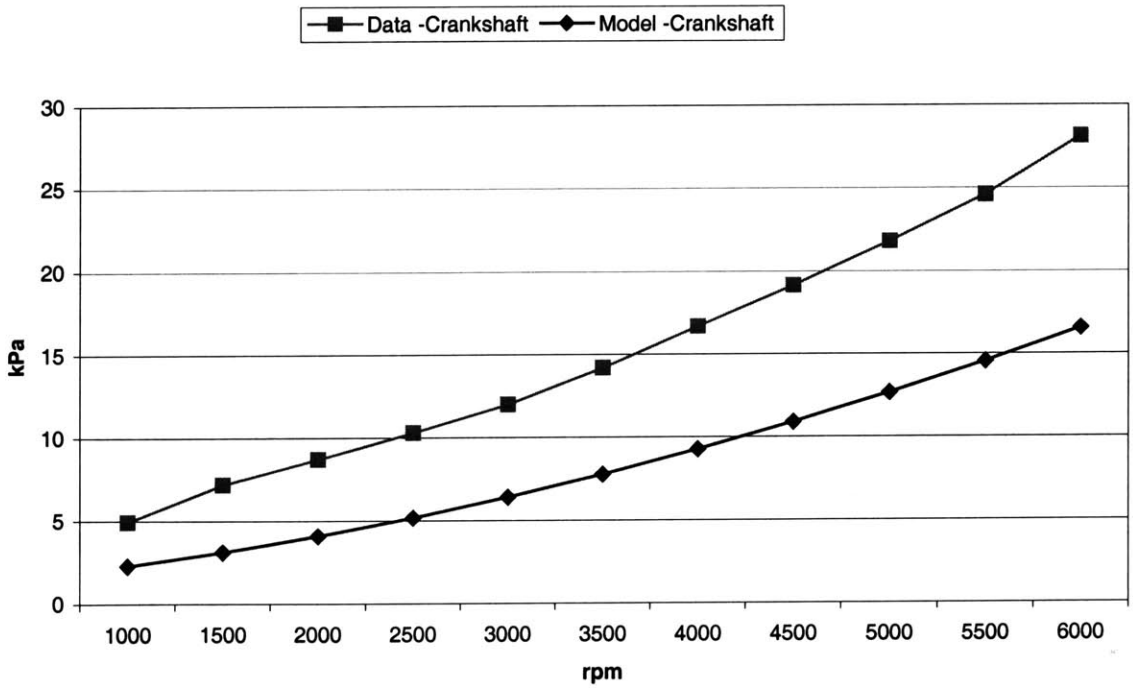

Figure 4-2: Comparison of crankshaft friction for 5.4L engine

4.3 Reciprocating Friction

4.3.1 Terms without Gas Pressure Loading

Figures 4-3 and 4-4, show the friction losses for the piston group (piston, piston rings, and connecting rod). The model for the 3.0L engine matched well during the low speed range and then fell a consistent amount below the data. At high speeds, the difference between the model and data was about 13 kPa. For this model, the piston ring hydrodynamic term dominated the friction contribution. The steep increase in the friction increased with speed, Equation 8.b, due to increasing piston velocity. The slight decrease in the data trend may have occurred due to the engine oil characteristics that were used when motoring the engine. The model for the 5.4L engine matched extremely well from low to high speed ranges. Again, the piston ring hydrodynamic term dominated the friction contribution as the friction increased due to the increase in mean piston speed.

This reciprocating model showed the similar increasing trend for the piston group friction. The data did not show such a trend. In the model, it is difficult to predict the dynamics of the tangential forces and lubrication characteristics at varying piston speeds. The model and data for the 5.4L engine showed the friction trend at various piston speeds, with an upward turn at 6000 rpm for the data.

4.3.2 Terms with Gas Pressure Loading

Data was not available to compare the gas pressure loading effect on the piston friction term because data has to be collected with the cylinder head and valvetrain mechanism. Figures 4-12 and 4-13, explained in section 4.6, include the gas exchange losses for the 3.0L and 5.4L engine.

4.4 Valvetrain Friction

Figures 4-5 and 4-6, show valvetrain friction losses for the 3.0L and 5.4L engine, respectively. In the 3.0L engine, the model over predicted the valvetrain friction, while in the 5.4L engine, the model under predicted the valvetrain friction. However, both models did maintain a similar trend to the engine data. The match between model and data fit well considering the flexibility of that the model had to predict friction for multiple types of interfaces. Table 4.2, shows the constants available for the different valvetrain mechanisms used in engines. A set of constants was added to the original table to be able to model the 3.0L engine. Existing constants were used to compare the 5.4L engine data.

The constants for the 3.0L DOHC finger follower valvetrain mechanism were obtained by matching the model to the engine data. The first three constants terms were kept the same as the

constants for a SOHC finger follower configuration. The oscillating mixed constant was set as 0.6 times the constant for the SOHC finger follower. This gave the best fit between data and model.

For the 5.4L engine, the difference at low and high engine speeds in the model may have been accounted for by the decrease in the boundary lubrication function term of 1 +1000/N to 1 +500/N. However, the data between the 2000 to 5000 rpm range matched extremely well.

Table 4.2: Constants for Valvetrain Mechanism Terms

TYPE	**Cam Follower Flat Roller**		**Oscillating Hydrodynamic**	**Oscillating Mixed**
SOHC finger follower	600	0.0227	0.2	42.8
SOHC rocker arm	400	0.0151	0.5	21.4
SOHC direct acting	200	0.0076	0.5	10.7
DOHC finger follower*	*600*	*0.0227*	*0.2*	*25.8*
DOHC direct acting	133	0.0050	0.5	10.7
OHV	400	0.5	0.5	32.1

*Determined to have improved model match engine data for DOHC finger follower valvetrain mechanisms.

4.5 Auxiliary Friction

Figures 4-7 and 4-8, show the accessory losses for the 3.0L and 5.4L engine, respectively. The auxiliary losses model indicates that there should be no differences between engines since accessory losses were only based on engine speed. The model for both engines fits the data well at speeds below 3500 rpm. For higher speeds, there is a sudden increase in the auxiliary losses based on the data. Although the characteristics of the accessories (oil pump, water pump, and alternator) were not studied, there are many friction losses that could have increased at higher speeds. There may have been high friction of the bearing and seals in the accessories at higher speeds. Also, the high hydraulic power that the oil and water pump produce, leads to an increase in the friction losses. For example, high-pressure losses occur in the narrow cross sections that the oil and water have to flow through.

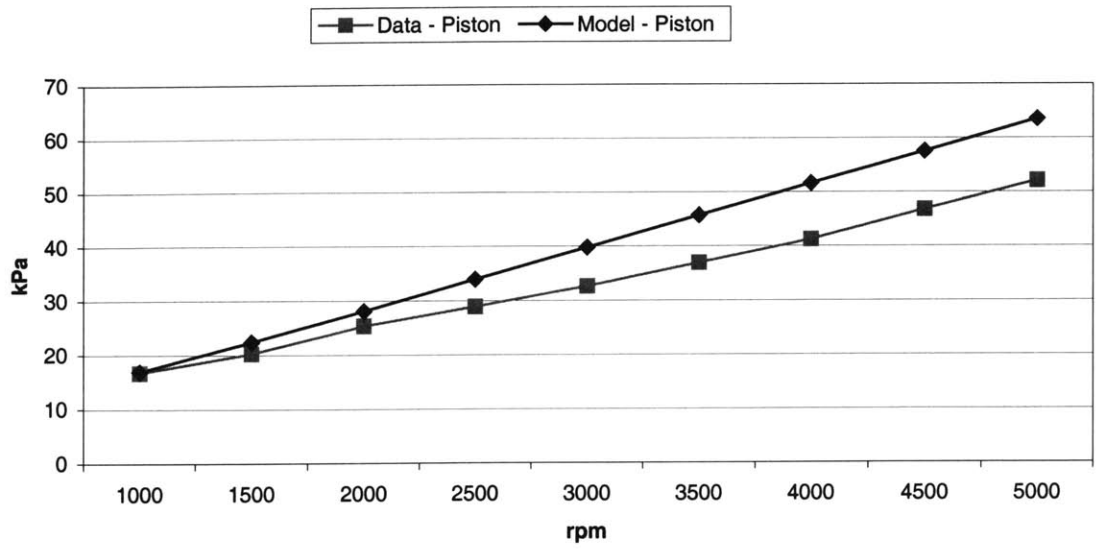

Figure 4-3: Comparison of reciprocating friction w/out gas for 3.0L engine

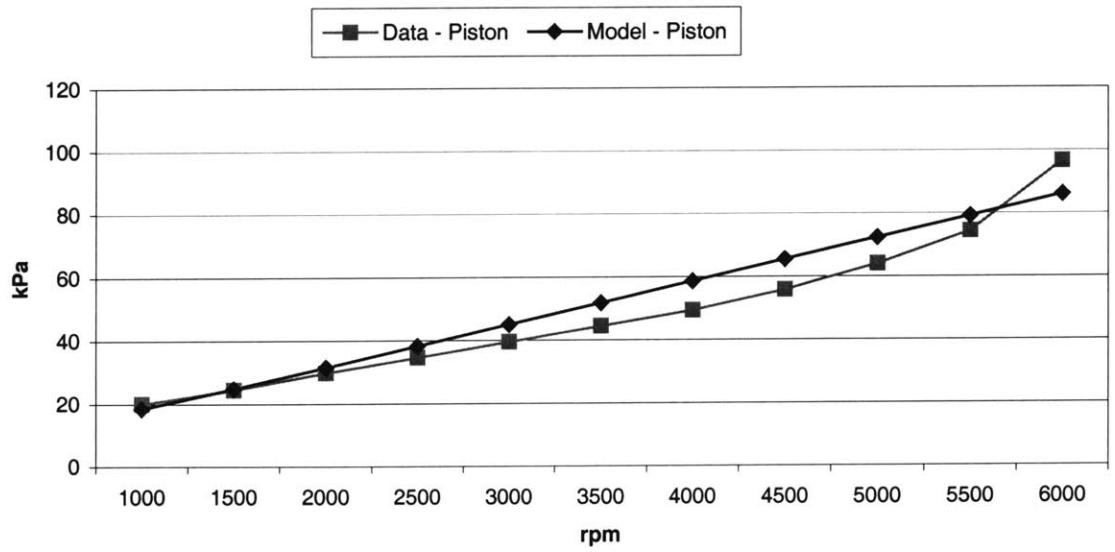

Figure 4-4: Comparison of reciprocating friction w/out gas for 5.4L engine

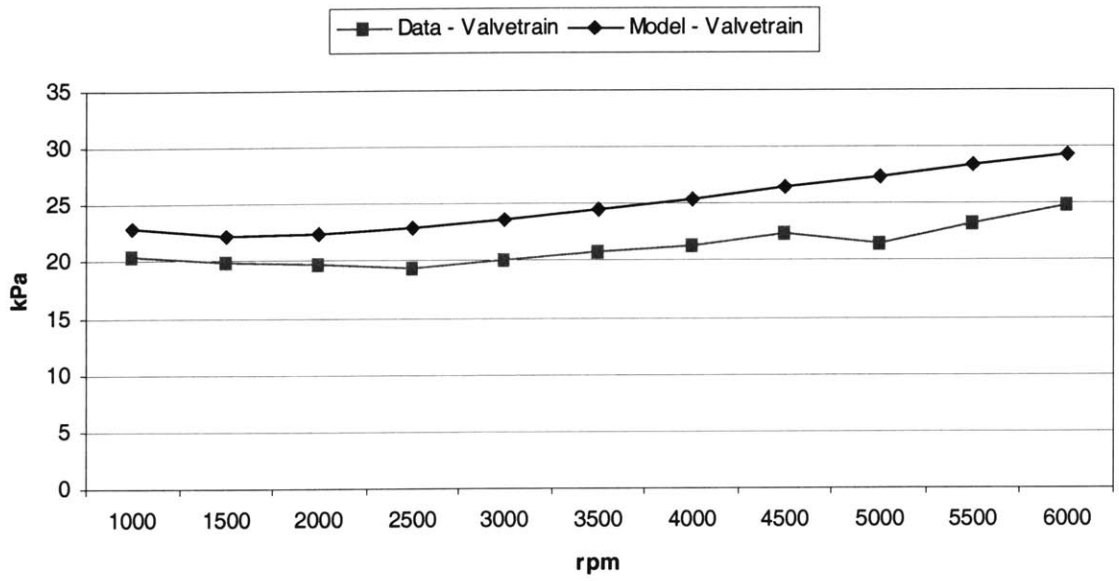

Figure 4-5: Comparison of valvetrain friction for 3.0L engine

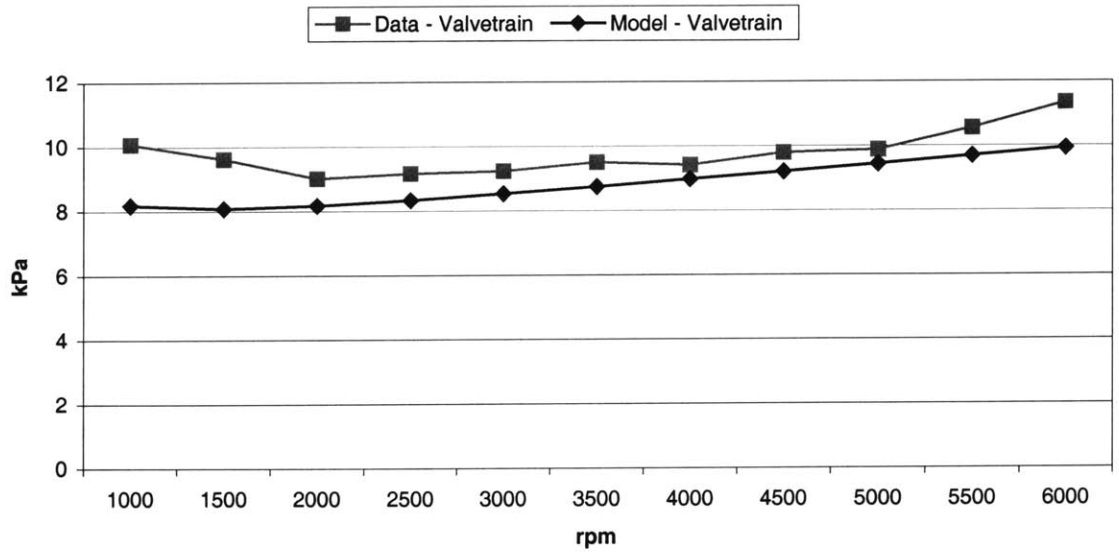

Figure 4-6: Comparison of valvetrain friction for 5.4L engine

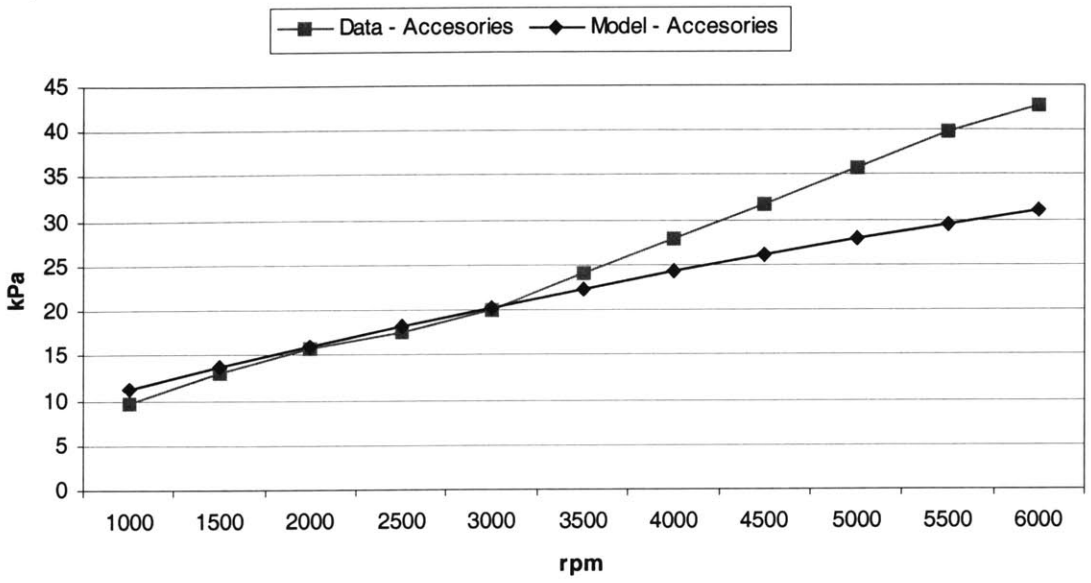

Figure 4-7: Comparison of accessory friction for 3.0L engine

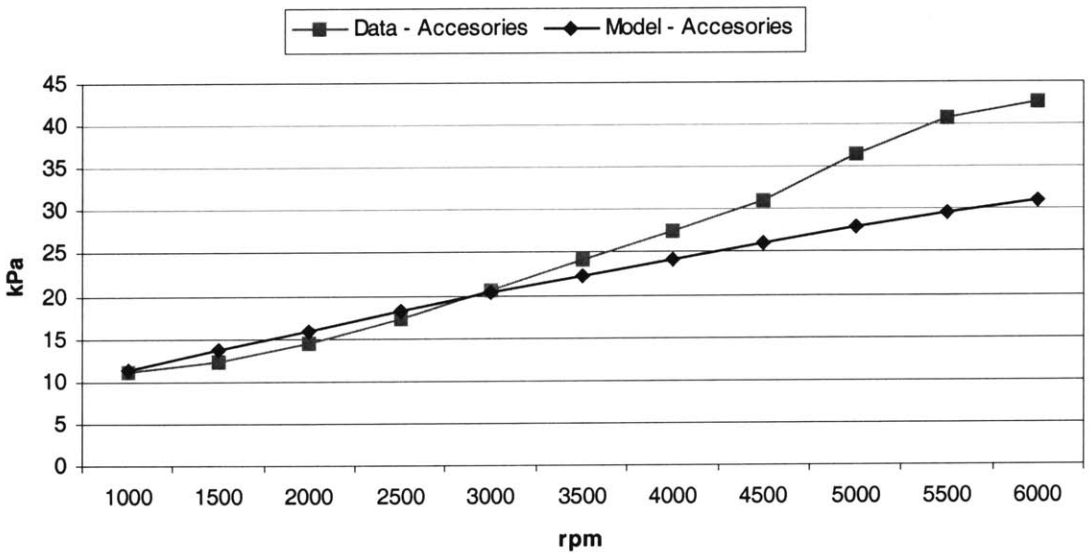

Figure 4-8: Comparison of accessory friction for 5.4L engine

4.6 Total Mechanical Losses

Figures 4-9 and 4-10, show the total mechanical friction obtained for the stripped engine tests for the 3.0L and 5.4L engines. This is the sum of the friction values for the crank train (crankshaft, piston group without gas pressure loading, connecting rod bearings), the valvetrain and accessories (oil pump, water pump, and unloaded alternator). The sum of the over and under prediction of the individual components gave a close match to the data. This makes the model suitable to predict total mechanical losses.

Figure 4-11, shows the result of the total mechanical friction obtained for the 6.8L prototype engine, tested under firing conditions. The model over predicts the mechanical friction by about 15 %, suggesting that continuing engine developments are leading to lower friction engines.

Figure 4-12, shows the result of the total mechanical friction with piston loading for the 3.0L engine. The model over predicted the frictional losses by an average of 15 kPa from low speeds to high speeds. However, both data sets follow the same trend. Again, the over and under prediction of the model for the mechanical losses may contribution to a total over prediction for the losses.

Figure 4-13, shows the result of the of the total friction losses for the 5.4L engine, including the intake and exhaust mean effective pressure. The model under predicts the data by about 10 kPa from low to high speeds, but follows a close trend with increasing speed. For this engine, the model gave an accurate match to the total actual friction losses. This gives an indication that the modifications made to the friction model reduced any over predictions that the previous model may have given.

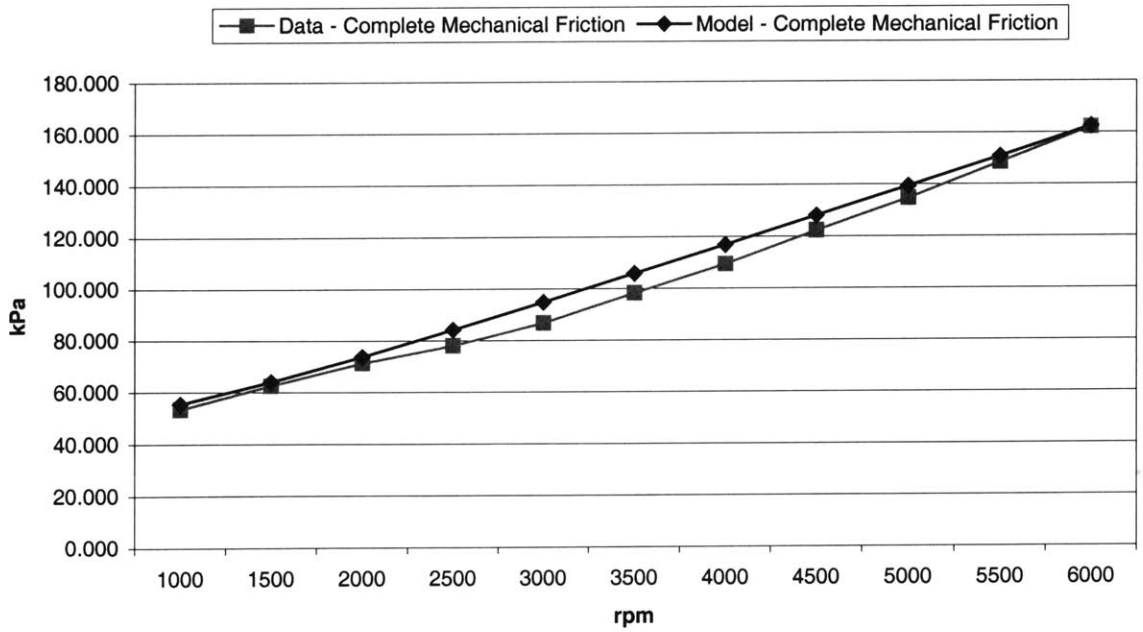

Figure 4-9: Comparison of complete mechanical friction for 3.0L engine

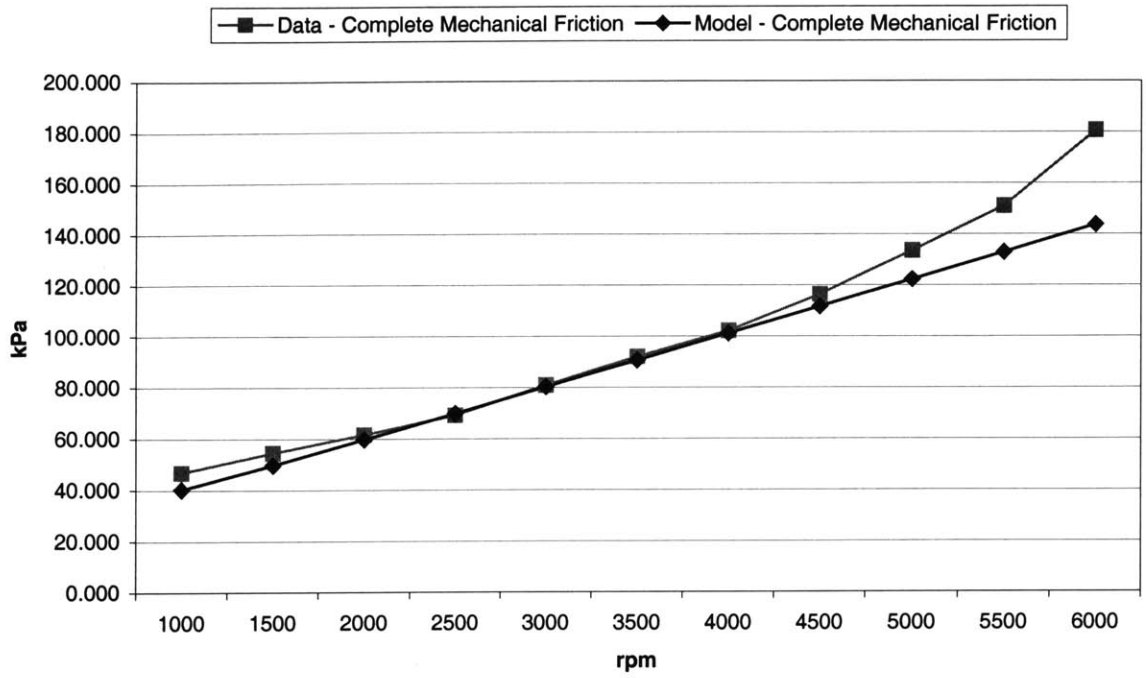

Figure 4-10: Comparison of complete mechanical friction for 5.4L engine

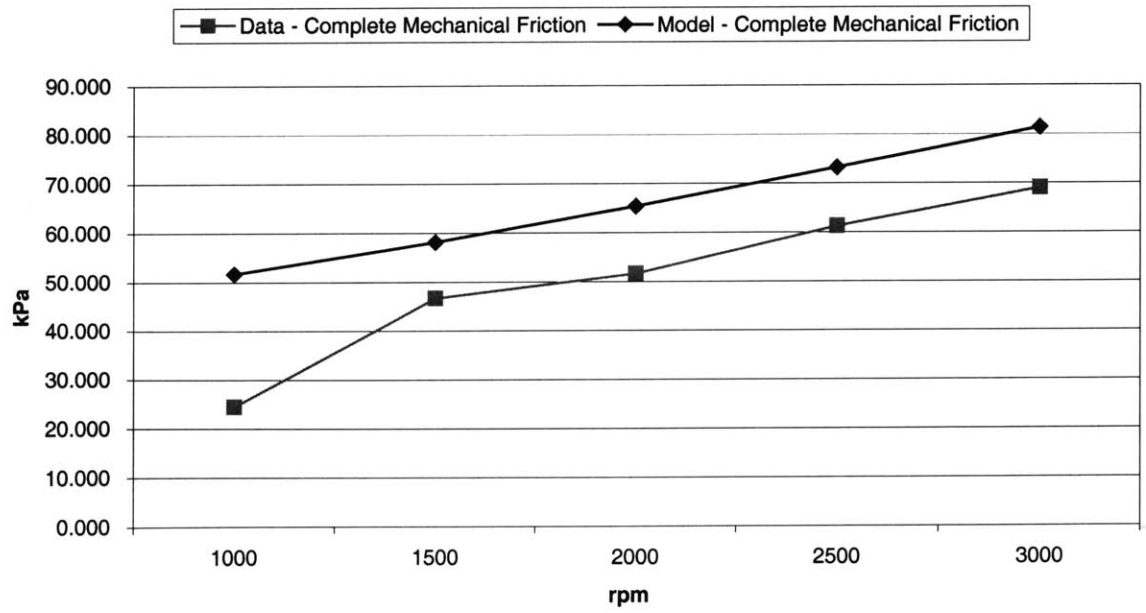

Figure 4-11: Comparison of complete mechanical friction for 6.8L at 55 kPA MAP

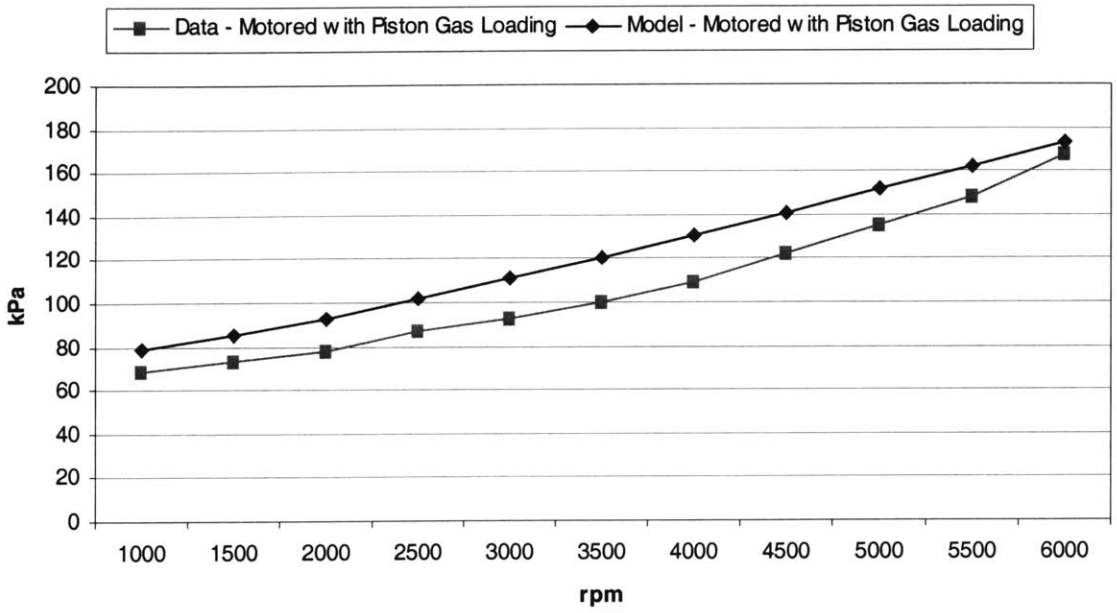

Figure 4-12: Comparison of total mechanical friction with piston gas loading for 3.0L engine

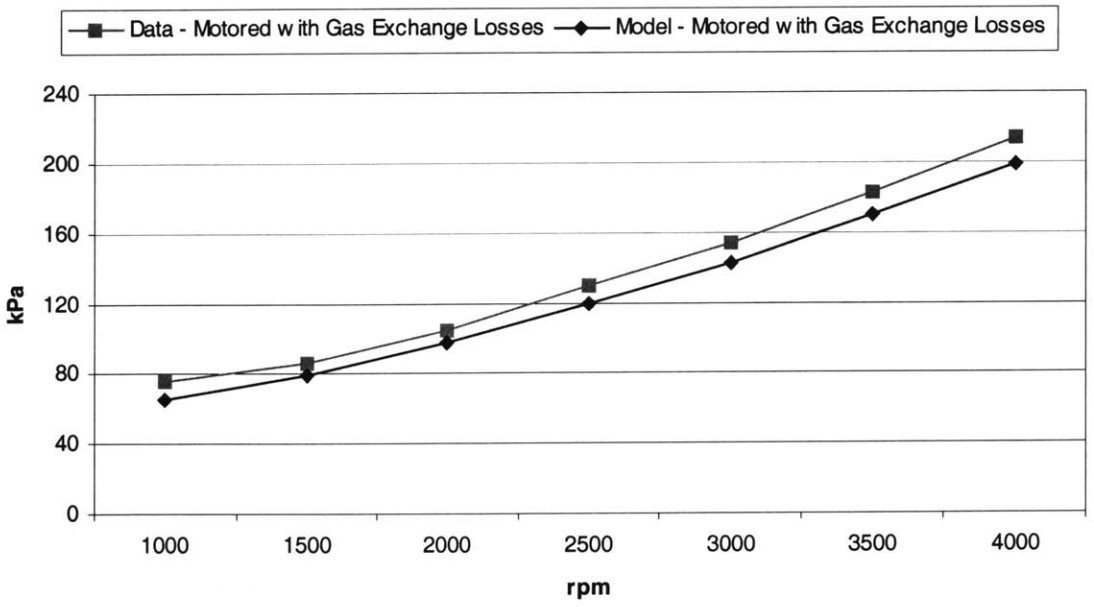

Figure 4-13: Comparison of total mechanical and gas exchange losses for 5.4L engine

4.7 Pumping Losses

Figure 4-14, shows the pumping losses for the 6.4L engine. This engine was used to verify the intake and exhaust friction mean effective pressure. The total pumping losses are the sum of the intake and exhaust system, and intake and exhaust valve pressure drop suggests the model oversimplifies the complexity of the intake and exhaust system. For this reason, the data was plotted for increasing intake map, mean atmospheric pressure, at constant speeds. The model shows the same trend for the pumping losses for increasing speeds and increasing map. At 1000 rpm, there is the largest difference between the model and the actual data. For increasing speeds, this difference decreases significantly and for 3000 rpm, the model matches the data fairly well. Also, at speeds higher than 2000 rpm, there is a slight kick in the model prediction caused by the pressure and mean piston squared terms. At higher speeds and maps, the exhaust system and both valve pressure drop terms have a higher contribution to the pumping losses.

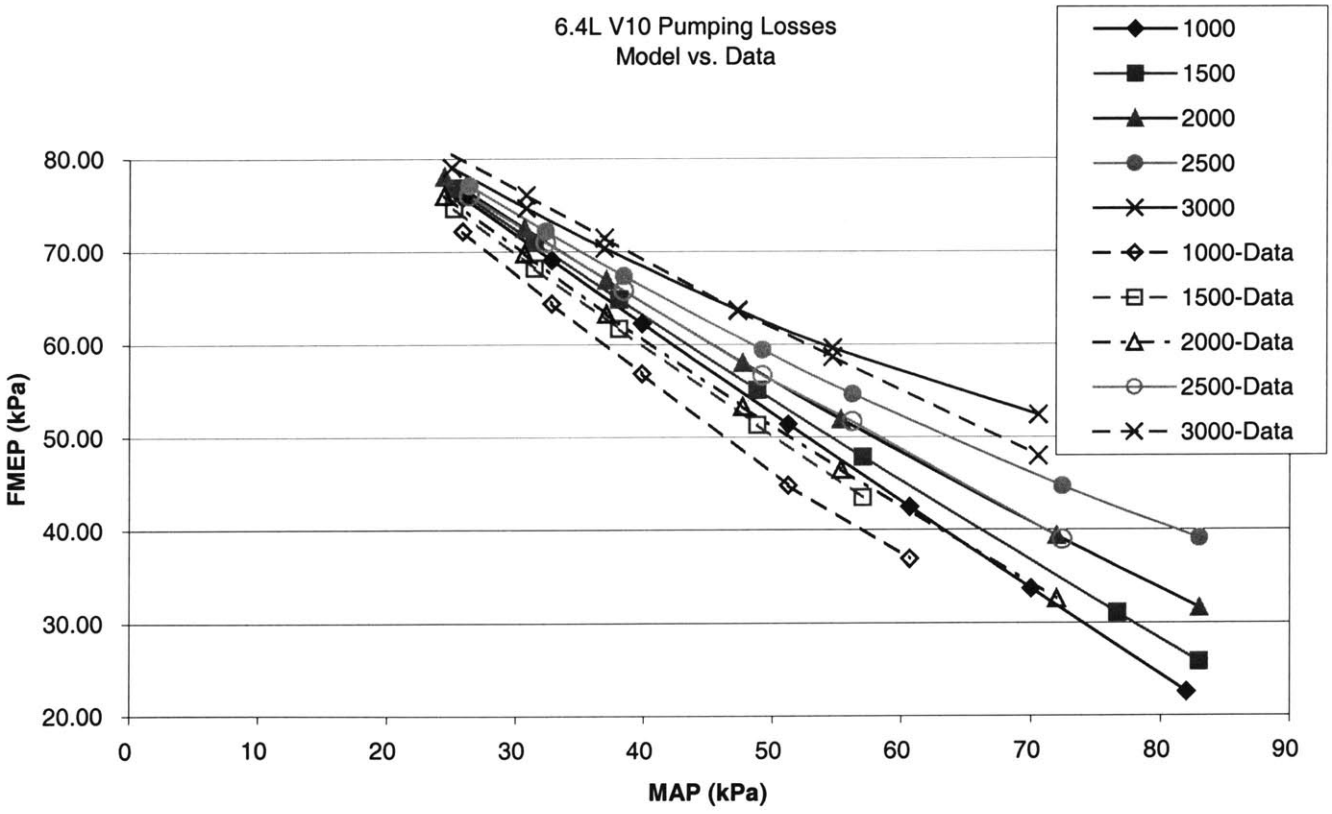

Figure 4-14: Comparison of Pumping Losses for 6.8L engine

4.8 Engine Warm Up

The viscosity scaling included in this model allowed us to see the effect of oil temperature on the different friction models. Shayler [10] included a modification in the previous Patton model to account for the increased friction losses, which arise during engine warm-up. These losses were attributed primarily to the effect of temperature on oil viscosity. In the test, the engine was allowed to soak down to room temperature (20°C) prior to each fired friction test. A plot of friction power loss against time from engine start was obtained. Several similar tests were carried out and all of these indicate that the friction power loss at engine start-up is over two times higher than the hot engine friction power loss.

With the modified friction model, data could now be collected given a particular temperature to calculate oil viscosity. Figures 4-15 and 4-16 show data that the model gave for different temperatures which affected the oil viscosity and therefore affected the friction terms. Comparing the total mechanical friction at 20 and 90°C shows a friction loss of about 2.1 times the hot engine friction power loss. This is comparable to the data that Shayler obtained from the firing tests.

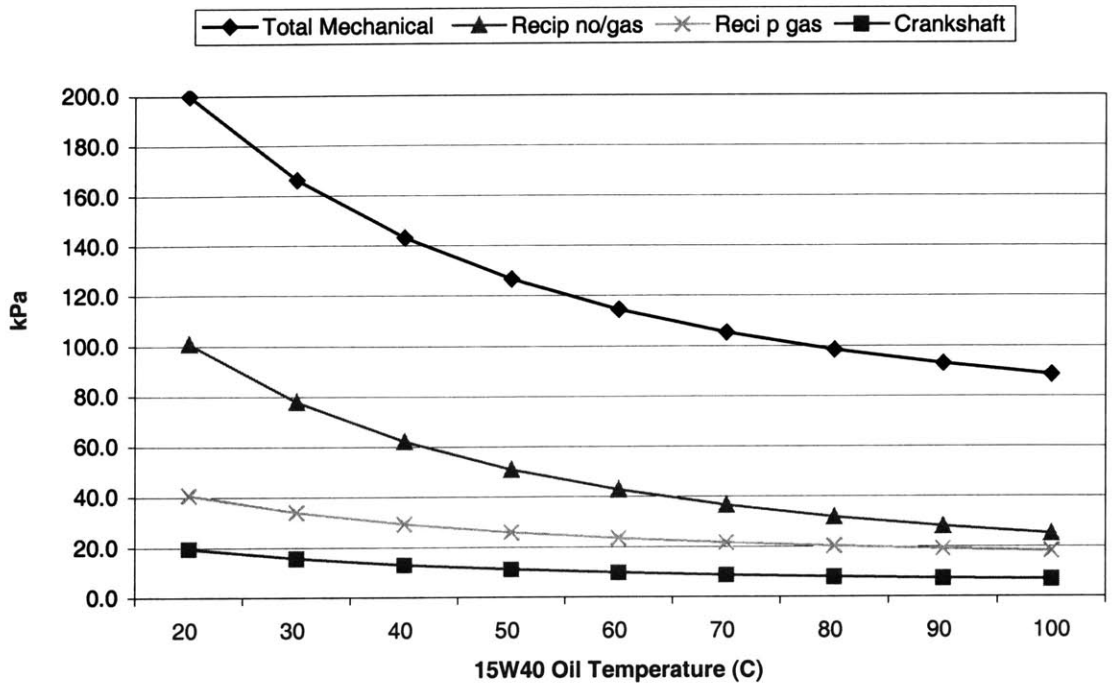

Figure 4-15: Friction for varying temperature at 2000 rpm for 3.0L engine

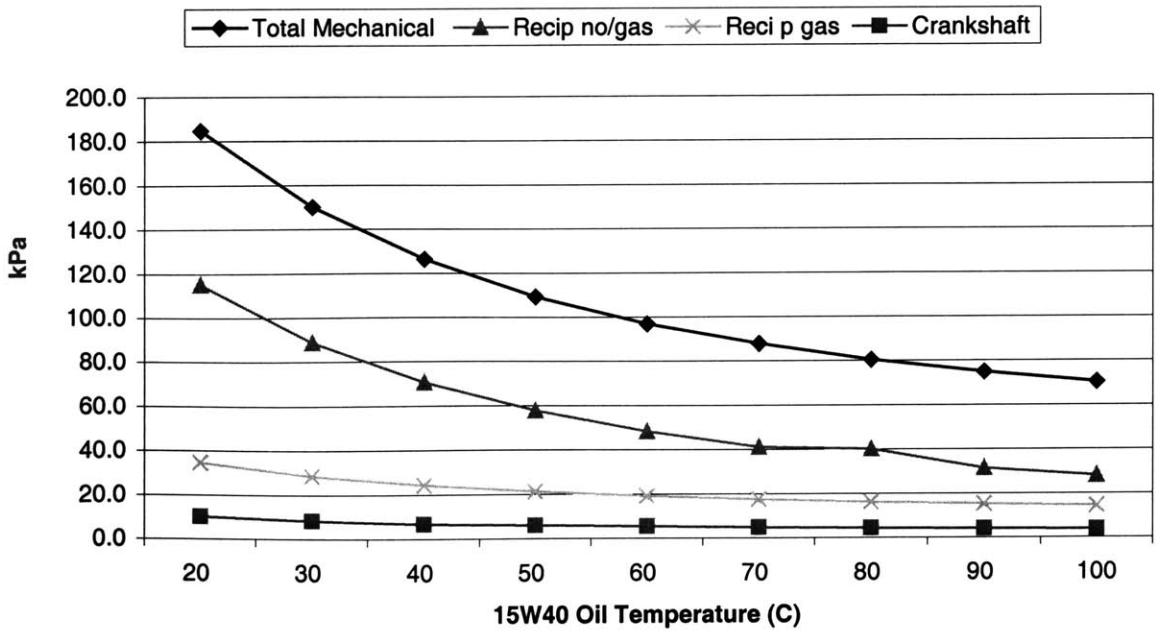

Figure 4-16: Friction for varying temperature at 2000 rpm for 5.4L engine

5 Summary

This paper documents the changes made to the Patton Friction Model to improve the predictive accuracy of the model. These changes were based using three engine data sets. The modifications were made knowing that the friction work components fell under three main categories; independent of speed (boundary lubrication), proportional to speed (hydrodynamic friction) or to speed squared (turbulent dissipation), or some combination of these. Modifications were made to the hydrodynamic terms to include their sensitivity to differences in oil grades and temperature. Changes to the boundary and turbulent terms were made knowing that engine design has changed to lower the total friction losses in an engine. Based on the model evaluation and subsequent use of the improved model, the following conclusion were drawn:

1. The experimental data shows that engine friction has decreased as engine design has improved. Main areas where model changes to reduce friction were piston friction and pumping losses.
2. More reliable predictions of crankshaft, reciprocating, valvetrain, and auxiliary friction and pumping losses can be made. The crankshaft and auxiliary friction models gave noticeable differences between model and data. The model under predicted crankshaft friction. For the auxiliary model, a constant difference was seen at speeds higher than 3500 rpm. However, the sum of the total friction losses gives an accurate prediction of the total engine friction.
3. The oil viscosity scaling with temperature allowed comparing the friction power loss from engine start to hot conditions. Comparing the total mechanical friction at 20 and 90°C showed a friction loss of about 2.1. This was comparable to the data that Shayler obtained from the firing tests.
4. The model now predicts, with acceptable accuracy, total friction and its major components in modern gasoline engines.

Bibliography

1. Wakuri, Y. et. al., Studies on Friction Characteristics of Reciprocating Engines, SAE Paper 952471.
2. Patton, K. J., Nitschke, R. G., and Heywood, J. B., Development and Evaluation of a Performance and Efficiency Model for Spark-Ignition Engines, SAE Paper 890836
3. Heywood J.B., "Internal Combustion Engine Fundamentals" *McGraw-Hill, New York,* 1988, pgs. 712-745.
4. Stribeck Diagram. http://www.egr.msu.edu/erl/case/sections/ch_07_26_02_d-3.htm
5. Stone, R.., "Introduction to Internal Combustion Engines" *Society of Automotive Engineers, Inc., Warrandale, Pa.,* 1999.
6. William, J.A., "Engineering Tribology" *Oxford University Press, New York, 1994*, pg. 241.
7. Chevron Supreme Motor Oil. http://library.cbest.chevron.com/lubes
8. Taylor, R. I., Brown, M.A., Thompson, D. M., and Bell, J. C., 1994, The Influence of Lubricant Rheology on Friction in the Piston Ring-Pack, SAE Paper 941981.
9. Tian, T., Modeling the performance of Piston Ring-Pack in Internal Combustion Engines, PhD Thesis, Department of Mechanical Engineering, MIT, June 1997.
10. Shayler, P.J., Christian, S.J., and Ma, T., A Model for the Investigation of Temperature, Heat Flow and Friction Characteristics During Engine Warm-up, SAE Paper 931153.
11. Cross-sectional view of an engine. http://www.howstuffworks.com

Appendix

A.1: Definition of Symbols

A	= area
afmep	= auxiliary friction mean effective pressure (kPa)
B	= bore (mm)
C	= radial journal bearing clearance
C_r	= piston roughness constant
cfmep	= crankshaft friction mean effective pressure (kPa)
D_b	= bearing diameter
D_v	= valve diameter (mm)
Δp	= pressure drop (kPa)
η_v	= volumetric efficiency
f	= friction coefficient
F_f	= friction force
fmep	= friction mean effective pressure (kPa)
F_n	= normal force
F_t/F_{to}	= piston ring tension ratio
L	= length
L_b	= bearing length (mm)
L_s	= piston skirt length
L_v	= maximum valve lift
$\dot{m}$	= mass flow rate
mfmep	= mechanical friction mean effective pressure (kPa)
μ	= oil viscosity
N	= engine speed (rpm)
n_b	= number of bearings
n_c	= number of cylinders
n_v	= number of valves
p_a	= atmospheric pressure (kPa)
p_i	= intake manifold pressure (kPa)
P_f	= friction power loss
pmep	= pumping mean effective pressure (kPa)
r_e	= exhaust valve diameter / bore
r_i	= intake valve diameter / bore
rfmep	= reciprocating friction mean effective pressure (kPa)
ρ	= density
S	= stroke (mm)
S_p	= mean piston speed (m/s)
tfmep	= total friction mean effective pressure (kPa)
V	= velocity
V_d	= displaced volume
vfmep	= valvetrain friction mean effective pressure (kPa)

A-1: Cross-section of an engine at intake stroke

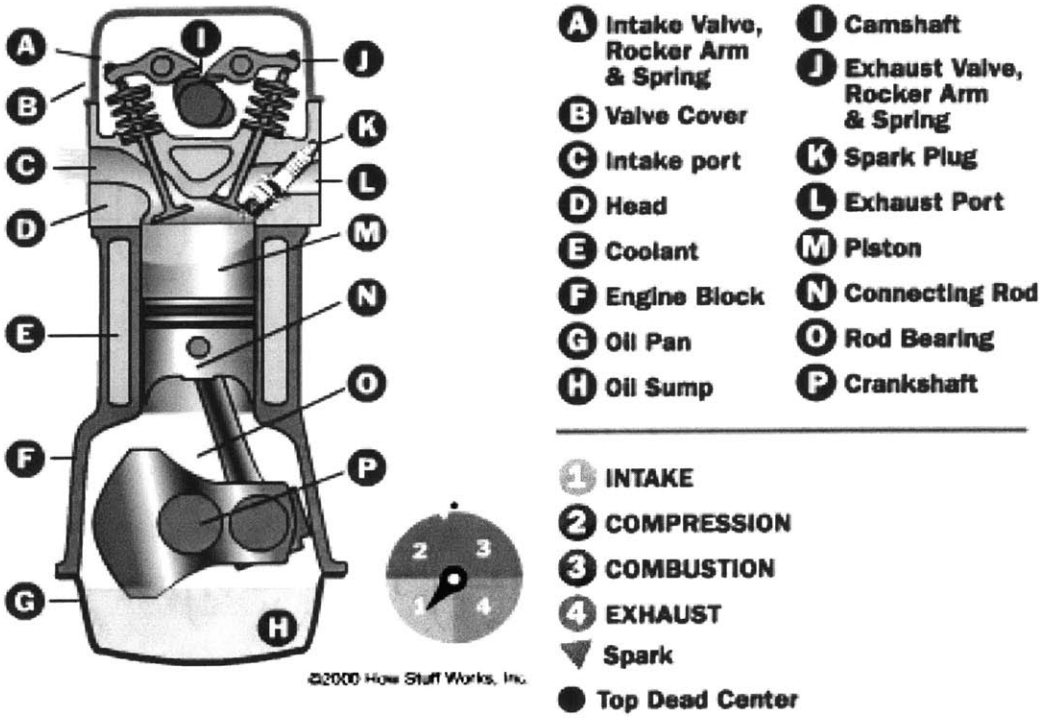

A.2: Oil Grades

Oil Grade	k **(cSt)**	θ_1 **(°C)**	θ_2 **(°C)**	μ_∞ / μ_0	c_1	c_2 **(°C^{-1})**
0W40	0.01341	1986.4	189.7	0.67	2.5	0.026
5W20	0.04576	1224	134.1	0.94	2.5	0.029
5W40	0.15	1018.74	125.91	0.8	2.3	0.0225
10W30	0.1403	869.72	104.4	0.76	2.3	0.0225
10W50A	0.0352	1658.88	163.54	0.49	2.43	0.0218
10W50B	0.0507	1362.4	129.8	0.52	2.28	0.0269
15W40A	0.1223	933.46	103.89	0.9	2.3	0.0225
15W40B	0.03435	1424.3	137.2	0.79	2.5	0.026
20W50	0.0639	1255.46	117.7	0.84	2.3	0.0225
SAE10	**0.0258**	**1345.42**	**144.58**	**1**	**2.3**	**0.0225**
SAE30	**0.0246**	**1432.29**	**132.94**	**1**	**2.3**	**0.0225**
SAE50	**0.0384**	**1349.94**	**115.16**	**1**	**2.3**	**0.0225**

A-2: Modified Expression for Total FMEP

An expression for total engine fmep, which is made up of all the component fmep terms, is:

$$fmep = 1.22\times10^{5}\left(\frac{D_b}{B^2Sn_c}\right)+3.03\times10^{-4}\sqrt{\frac{\mu}{\mu_o}}\left(\frac{ND_b^3L_bn_b}{B^2Sn_c}\right)+1.35\times10^{-10}\left(\frac{D_b^2N^2n_b}{n_c}\right)$$

$$+2.94\times10^{2}\sqrt{\frac{\mu}{\mu_O}}\left(\frac{S_p}{B}\right)+4.06\times10^{4}\left(\frac{F_t}{F_{to}}C_r\right)\left(1+\frac{500}{N}\right)\left(\frac{1}{B^2}\right)+3.03\times10^{-4}\sqrt{\frac{\mu}{\mu_O}}\left(\frac{ND_b^3L_bn_b}{B^2Sn_c}\right)$$

$$+6.89\frac{p_i}{p_a}\left[0.088\sqrt{\frac{\mu}{\mu_O}}r_c+0.182\left(\frac{F_t}{F_{to}}\right)r_c^{(1.33-2KS_p)}\right]+4.12$$

$$+244\sqrt{\frac{\mu}{\mu_o}}\frac{Nn_b}{B^2Sn_c}+C_{ff}\left(1+\frac{500}{N}\right)\frac{n_v}{Sn_c}+C_{rf}\left(\frac{Nn_v}{Sn_c}\right)$$

$$+C_{oh}\sqrt{\frac{\mu}{\mu_o}}\left(\frac{L_v^{1.5}N^{0.5}n_v}{BSn_c}\right)+C_{om}\left(1+\frac{500}{N}\right)\frac{L_vn_v}{Sn_c}$$

$$+6.23+5.22\times10^{-3}N-1.79\times10^{-7}N^2$$

$$+(p_a-p_i)+3.0\times10^{-3}\left(\frac{p_i}{p_a}\right)^2\left(\frac{S_p^2}{n_v^2r_i^4}\right)$$

$$+0.178\left(\frac{p_i}{p_a}S_p\right)^2+3.0\times10^{-3}\left(\frac{p_i}{p_a}\right)^2\left(\frac{S_p^2}{n_v^2r_e^4}\right)$$

K is equal to 2.38 x 10^{-2}, and C_{ff}, C_{rf}, C_{oh}, C_{om} are constants based on the valvetrain mechanism.

A.3: Sample Input Configuration for Friction Model

6	NCYL - NUMBER OF CYLINDERS
2	BLKCON - 1/2 : LINE/VEE BLOCK CONFIGURATION
2	BLKMTL - 1/2 : IRON/ALUM BLOCK MATERIAL
3	VLVCON - 1/2/3 : OHV/SOHC/DOHC VALVETRAIN CONFIGURATION
2	FOLTYP - 1/2 : FLAT/ROLLER FOLLOWER TYPE
2	VLVMEK - 1/2/3 : ROCKARM/FINGFOL/DIRACT VALVETRAIN MECHANISM
6.0	IVO - INTAKE VALVE OPENING POINT (deg-CA BTDC)
236.0	IVDUR - INTAKE VALVE OPEN DURATION (deg-CA)
50.0	EVO - EXHAUST VALVE OPENING POINT (deg-CA BBDC)
245.0	EVDUR - EXHAUST VALVE OPEN DURATION (deg-CA)
1	WOTSWITCH (WIDE OPEN THROTTLE = 1)
1	TUNSWITCH (TUNED=1)
1	MOTSWITCH (MOTORING=1)
1	intake valves
1	exhaust valves
33.8	intake valve diameter (mm)
37.5	exhaust valve diameter (mm)
0.37978	iv/bore
0.42135	ev/bore
15W40	Oil Type (0W40,5W20,5W40,10W30,10W50,15W40)
90	Temperature (Celsius)
14.326	Viscosity (cSt at 100C)
10.3	Reference viscosity (cSt at 90C)
1.3908	Ratio of viscosity